Design and Evaluation of W and D Band TUNNETT Devices [1]

C. Kidner, G. I. Haddad, J. R. East and H. Eisele
Solid-State Electronics Laboratory
Department of Electrical Engineering and Computer Science
University of Michigan
Ann Arbor, Michigan, 48109-2122

Abstract

Preliminary estimates of the power generation capability of Tunnel Transit Time (TUNNETT) devices in the 100-1000 GHz range are promising. A straight forward TUNNETT design procedure based on experimental characterization of the tunnel injector is outlined. A GaAs tunnel injector has been characterized and a nominal 100 GHz design is given. Preliminary results for tunnel injectors using InGaAs lattice matched to InP are described. The Gilden and Hines small signal analysis of transit time devices is modified and applied to TUNNETT devices. The RC time constant of the tunnel injector is shown to be an important figure of merit.

[1]This work was supported by the Center for Space Terahertz Technology under contract No. NAGW-1334

1. Introduction

Two terminal transit time devices are strong candidates for high frequency power generation. IMPATT devices have demonstrated high power capabilities for frequencies up to 100 GHz. The technology at higher frequencies is not as mature, but preliminary work is promising [1–4]. At very high frequencies IMPATTTs are expected to give way to MITATTs and TUNNETTs as fundamental sources. Transit time devices are also attractive due to their relatively simple biasing requirements. Since they do not have intrinsic negative resistance at low frequencies it is relatively simple to suppress bias circuit oscillations.

While IMPATTs are useful devices, they do have limitations. Due to the avalanche multiplication, shot noise in IMPATTs may be relatively high. Devices based on the avalanche process also suffer a significant decrease in efficiency at extremely high frequencies. IMPATTs are also limited because at higher frequencies the narrow active region and high doping level required lead to tunneling mechanisms becoming dominant.

TUNNETTs and MITATTs take advantage of the very fast and relatively quiet tunneling process. These devices are expected to produce significant power at extremely high frequencies. Such devices have been considered previously [5–8] and preliminary experimental results have been obtained in the 100-300 GHz range. Recent advances in material growth and processing technology will greatly improve the performance attainable from these devices.

This paper discusses the basic design and evaluation of TUNNETT devices. First order estimates of the power generation capabilities of TUNNETTs are presented using simple large signal techniques. We then discuss a procedure for designing TUNNETT structures. The design is based on the experimental characterization of the tunnel injector. Characteristics of GaAs and InGaAs injectors are presented and a 94 GHz TUNNETT design based on the GaAs injector is presented. A small signal analysis of TUNNETT structures is carried out by modifying the analysis Gilden and Hines performed on IMPATT diodes [9]. Simple expressions for the real and imaginary parts of

the device impedance are derived. The small signal results show the importance of the tunneling injector in the device operation.

2. Estimation of Expected Power Output From Conventional Single-Drift TUNNETT Devices

The TUNNETT structure we consider is shown schematically in Fig. 1. The devices of interest here will be punched through at the bias voltage and the device is designed to maintain a high field in the drift region. Under these conditions we can assume that the length of the depletion region, x_D is constant and the injected charge travels at v_s, where v_s = the saturated velocity.

The analysis is a simplified first order theory meant to give order of magnitude estimates. Details of the analysis are given in [10]. The effects of the series resistance associated with a realistic device were included and limitations due to power dissipation were also considered. The results of the analysis are given in Tables I–III for 100 GHz, 500 GHz and 1000 GHz, respectively. The analysis predicts useful power can be generated using TUNNETT devices. It can be seen from these tables that for all the cases considered except for one, the temperature rise does not exceed 225 K and therefore CW operation is feasible for these cases.

3. Design of Single-Drift TUNNETT Devices

We have developed a first order TUNNETT design prodedure which will result in a working device so that experimental studies may be carried out. The design is based on an experimental characterization of the tunnel injector. The design procedure ignores some second order effects which will be important for more optimal designs. We conclude the section with the design of a nominal 100 GHz TUNNETT using MBE grown GaAs layers.

For TUNNETT devices the optimum transit angle is $\omega\tau_D = \frac{3\pi}{2}$ and thus the drift

region length (see Fig. 1) is

$$x_D = \frac{3v_s}{4f} \quad . \tag{1}$$

It is important to keep carrier generation in the drift region low. Since the drift region is relatively long carrier generation through impact ionization can be significant. We will therefore require that

$$\int_0^{x_D} \alpha \, dx = 0.1 \tag{2}$$

where α = ionization rate = $Ae^{-(b/E)^m}$. A and b are material parameters.
For a given frequency of operation x_D is known. The magnitude of the electric field at x_D for dc bias is chosen to give saturated velocity and to keep the diffusion coefficient low. The ionization multiplication factor is found numerically for different doping levels in the drift region given an assumed $E(x_D)$. Values for a 100 GHz GaAs design are presented later.

It is difficult to accurately characterize the tunnel injector from simple theory. The basic form of the current generation as a function of the electric field is well known [11] and is expressed as

$$G_T(E) = A_T E^2 \exp\left(\frac{-B_T}{E}\right) \quad . \tag{3}$$

The constants can be found using a highly idealized analysis to be

$$A_T = \frac{1}{2\pi^2}\left[\frac{E_g}{2\pi\hbar}\right]\left[\frac{q}{E_g}\right]^2\left[\frac{2M_r^* E_g}{\hbar^2}\right]^{1/2} \tag{4}$$

and

$$B_T = \frac{\pi}{4}\left[\frac{E_g}{2\pi\hbar}\right]\left[\frac{2M_r^* E_g}{\hbar^2}\right]^{1/2} \tag{5}$$

where E_g is the semiconductor bandgap energy and M_r^* is the effective tunneling mass given by

$$M_r^* = \frac{M_c^* M_v^*}{M_c^* + M_v^*} \quad . \tag{6}$$

In eq. 6 M_c^* is the conduction band effective mass and M_v^* is the valance band effective mass. For accurate characterization of a real semiconductor material, however, the parameters A_T and B_T will require measurements.

For a first order design of a GaAs TUNNETT injector accurate knowledge of A_T and B_T is not required. In GaAs the bandgap energy is large enough that for the desired tunnel current the highest doping levels available are required. With current MBE technology this results in a one sided p^+n junction: $N_A = 5.0 \times 10^{19}/\text{cm}^3$ and $N_D = 5.0 \times 10^{18}/\text{cm}^3$. The only parameter to be calculated is the width of the highly doped n-type region, x_A. The desired dc current density is known from the large signal analysis. By measuring the zero bias capacitance and the bias required to give the correct current density in a p^+n junction without the drift region the magnitude of the field at the p^+n junction necessary to produce this current density is calculated using

$$E_{max} = \frac{qN_D}{A} C_0 \left[\frac{V_{bi} - V_A}{V_{bi}}\right]^2 \tag{7}$$

where N_D is the doping concentration, V_{bi} is the built in voltage (estimated from the forward biased IV characteristic), V_A is the applied voltage, A is the area of the diode and C_0 is the zero bias capacitance of the diode. The magnitude of the electric field at the beginning of the drift region is determined from the doping level and the length of the drift region. Thus the length of the highly doped n-type region is

$$x_A = (E_{max} - E_{drift}) \frac{\epsilon_r \epsilon_0}{qN_D} \quad . \tag{8}$$

For an InGaAs injector the situation is more complex. Due to the smaller bandgap energy the tunnel breakdown voltage of the injector can be made extremely small with doping levels using current MBE technology. In order to determine the optimum doping level available InGaAs (lattice matched to InP) p^+n^+ junctions with various nominal n^+ doping levels are being studied using MBE and gas source MBE grown material. Both growth technologies are available at our laboratory. MBE grown material with nominal doping levels of $p^+ : N_A = 1 \times 10^{19}/\text{cm}^3$ and $n^+ : N_D = \{3 \times 10^{18}/\text{cm}^3, 1 \times 10^{18}/\text{cm}^3, 3 \times 10^{17}/\text{cm}^3, 1 \times 10^{17}/\text{cm}^3\}$ have been processed into diodes. The IV curves of 90μm diameter diodes are given in Fig. 2. Higher doping levels are available with this system than those used for this study. The IV curve of a gas source MBE grown sample with nominal doping levels of $N_A = 1 \times 10^{19}/\text{cm}^3$ and

$N_D = 1\times10^{19}/\text{cm}^3$ is shown in Fig. 3. The InGaAs samples will require careful evaluation in order to give accurate estimates of the tunneling parameters A_T and B_T. A comparison of the growth techniques is under way to determine which technique is more suitable for growing TUNNETT structures.

This design procedure has been used to specify a 100 GHz (nominal) TUNNETT structure in GaAs. The electrons travel at the saturated velocity of $v_s = 10^7$ cm/s in the drift region so

$$x_D = \frac{3v_s}{4f} = 0.75\mu\text{m} \quad . \tag{9}$$

The desired field strength at the end of the drift region ($E(x_D)$) is estimated to be 100kV/cm from large signal analysis and experience with similar devices. The doping level in the drift region should be as large as possible to minimize distortions of the field profile due to the injected charge. The upper limit to the doping level is the level determined by imposing an upper limit on the impact ionization multiplication factor. For GaAs $A_i = 3.85\times10^5$/cm, $b = 6.85\times10^5$ V/cm and $m = 2$ was used. Numerically integrating eq. 2 gives a maximum doping of $N_D = 3.0\times10^{16}/\text{cm}^3$. Since the magnitude of the field at the end of the drift region (100 kV/cm), the length of the drift region (0.75μm), and the charge density in the drift region (qN_D) are known, Poisson's equation can be used to estimate the magnitude of the electric field at the beginning of the drift region to be E(0)=400k V/cm. The required current density is known from the large signal analysis to be 30 kA/cm^2. We estimate that the maximum field at the junction to be 3.23 MV/cm by characterizing the tunnel injector without a drift region and using eq. 7. The desired width of the n^+ side of the tunnel injector is calculated to be 403Å using eq. 8. If the doping level in the injector is lower than the nominal the field in the drift region will cause excessive impact ionization. To avoid this we specified the injector to be slightly longer; 420Å. This structure was grown by a source outside the University of Michigan. The doping levels of the resulting structure measured using SIMS are shown in Fig. 4. Note the Si (n-type) doping profile, particularly in the injector region, is excellent. The cause of the failure of the Be (p-type) doping is thought to be understood. A new sample has been grown and is currently being tested using SIMS analysis.

4. Small Signal Analysis of TUNNETTs

The small signal analysis of the TUNNETT follows the analysis performed by Gilden and Hines for IMPATT devices. The most important difference is that the tunnel injector is modeled as a parallel R–C circuit rather than a parallel L–C circuit, see Fig. 5. The impedance of the tunnel injector is (compare to eq. (14) in [9])

$$Z_a = \frac{R}{1 + j\omega RC_a} \tag{10}$$

while the impedance of the drift region is (compare with eq. (18) in [9])

$$Z_d = \frac{1}{j\omega C_d}\left\{1 - \frac{1}{1 + j\omega RC_a}\left(\frac{\sin\Theta}{\Theta} - j\frac{1-\cos\Theta}{\Theta}\right)\right\} \quad . \tag{11}$$

Where $R = 1/G$ = dc small signal resistance ($\Delta V/\Delta I$) of the tunnel injector. C_a = junction capacitance of the injector ($\epsilon A/x_A$). C_d = drift region capacitance ($\epsilon A/x_D$). Θ = transit angle of the drift region ($\omega x_D/v_s$). Following the analysis through for the TUNNETT case results in the small signal impedance of the device being (Z_T=R_T+jX_T)

$$R_T = \frac{\omega RC_a \sin\Theta + 1 - \cos\Theta + \omega C_d \Theta R}{\Theta\omega C_d(1 + \omega^2 R^2 C_a^2)} \tag{12}$$

$$X_T = \frac{\sin\Theta - \Theta - R\omega C_a(1 - \cos\Theta) - \Theta\omega^2 R^2 C_a(C_a + C_d)}{\omega\Theta C_d(1 + \omega^2 R^2 C_a^2)} \quad . \tag{13}$$

The denominator of both terms contains the term $1 + \omega^2 R^2 C_a^2$ which implies that the RC time constant of the tunnel injector is an important figure of merit when considering a design for high frequency oscillations.

For a TUNNETT device operating at its optimum frequency ($\Theta = \frac{3}{2}\pi$),the equation for the real part of the impedance becomes

$$R_T = \frac{-\omega RC_a + 1 + \omega C_d R\Theta}{\omega C_d \Theta\,(1 + \omega^2 R^2 C_a^2)} \quad . \tag{14}$$

For very high frequencies

$$\lim_{\omega\to\infty}(R_T) = -\frac{1}{\omega^2 C_d RC_a} \quad . \tag{15}$$

Note that since C_d is proportional to the desired operating frequency the negative resistance will drop off as the cube of the frequency. The resistance of the diode is positive

for $\omega < 1/RC_a$, so a TUNNETT will not begin oscillations below the cutoff frequency of the injector. Fortunately, the small signal resistance of the injector increases as the current density is decreased. So injectors with very high cutoff frequencies can be made to operate simply by reducing the current density.

There is some ambiguity to the separate values of R and C_a since the length of the tunnel injection region is not well defined. The RC product, however, is easily obtained from low frequency measurements performed on a simple pn junction. The rate of tunnel injection varies exponentially with the electric field so it is a very close approximation to assume that the tunnel injection region is very short. Also, if space charge effects in the injector are ignored the small signal electric field is constant across the injector region. Then the small signal voltage across the injector is directly proportional to the assumed length of the injector region. Thus if the assumed length of the injector is longer than the real length of the injector (so that the current density appears independent of the length of the injector) the small signal resistance ($\frac{\partial V}{\partial I}$) is directly proportional to the assumed length. Since the capacitance is inversely proportional to the length, the RC time constant is independent of the assumed length of the injection region. So the small signal RC time constant measured using the pn junction alone is the same as that of the injector. The ambiguity in the value of R will have little effect since the $\omega C_d R \Theta$ term is small compared to the other terms for the frequencies considered here.

For the GaAs tunnel injector studied biased to give a current density of 30 kA/cm^2 the measured values were $R = 1.5\Omega$, $C_a = 5.0\,pF$, $RC_a = 7.67\,pS$. Since the resistance value is small and had to be measured at a high current value it could not be measured precisely. The measured value includes a series resistance associated with the measurement system which is of the order of half an ohm. It also includes the contact resistance, which is small, since the diodes are large. The above value is in the range expected from the standard tunneling theory. The measured value is thought to overestimate the RC time constant and should only be considered as a first order estimate. The measured value implies the 3 dB frequency for this injector is 21 GHz. The small signal impedance of the nominal 100 GHz GaAs TUNNETT design given in section 3 as a function of frequency

is shown in Fig. 6. The small signal impedance of a TUNNETT structure designed for 500 GHz is given in Fig. 7.

5. Conclusions

Preliminary estimates of the power generation capability of TUNNETT devices in the 100-1000 GHz range are promising. A straight forward TUNNETT design procedure based on experimental characterization of the tunnel injector has been outlined. A GaAs tunnel injector has been characterized and a nominal 100 GHz design has been given. Preliminary results for tunnel injectors using InGaAs lattice matched to InP has been carried out and the results are promising. The Gilden and Hines small signal analysis of transit time devices has been modified for TUNNETT devices. The RC time constant of the tunnel injector was shown to be an important figure of merit, though the injector is useful far above its cutoff frequency. It is believed that useful power at one terahertz is feasible using TUNNETT structures.

Acknowledgments The authors are grateful to Dr. W. Q. Li and Prof. P. Bhattacharya of the University of Michigan for providing the MBE InGaAs material. They are also grateful to M. Sherwin and G. Munns, both at the University of Michigan, for the gas source MBE InGaAs material.

REFERENCES

[1] W. T. Read, "A Proposed High-Frequency Negative Resistance Diode," *Bell Syst. Tech. J.*, vol. 37, (1958), p. 401.

[2] R. K. Mains and G. I. Haddad, "Properties and Capabilities of Millimeter-Wave IMPATT Diodes," *Infrared and Millimeter-Waves*, K. J. Button (Ed.), vol. 10, Part III, Chap. 3, Academic Press, Inc., New York, 1983.

[3] R. K. Mains, G. I. Haddad and P. A. Blakey, "Simulation of GaAs IMPATT Diodes Including Energy and Velocity Transport Equations," *IEEE Trans. on Electron Devices,* vol. Ed-30, No. 10, October 1983, pp. 1327–1338.

[4] H. Eisele and H. Grothe, "GaAs W-band IMPATT diodes made by MBE", *Proc. MIOP '89*, Sindelfingen, FRG, Feb. 28–March 3rd 1989, Session 3 A.6.

[5] J. Nishizawa, K. Mofoya and Y. Okuno, "GaAs TUNNETT Diodes," *IEEE Trans. on Microwave Theory and Techniques*, vol. MTT-20, No. 12, December 1978, pp. 1029–1035.

[6] M. Elta and G. I. Haddad, "High-Frequency Limitations of IMPATT, MITATT, and TUNNETT Mode Devices," (invited paper) *IEEE Trans. on Microwave Theory and Techniques*, vol. MTT-27, No. 5, May 1979, pp. 442–449.

[7] M. E. Elta, H. R. Fetterman, W. V. Macropoulas and J. J. Lambert, "150 GHz GaAs MITATT Source," *IEEE Electron Device Letters,* vol. EDL-1, No. 6, June 1980, pp. 115–116.

[8] N. S. Dogan, J. R. East, M. E. Elta and G. I. Haddad, "Millimeter-Wave Heterojunction MITATT Diodes," *IEEE Trans. on Microwave Theory and Techniques*, vol. MTT-35, No. 12, December 1987, pp. 1308–1317.

[9] M. Gilden and M. E. Hines, "Electronic Tuning Effects in the Read Microwave Avalanche Diode," *IEEE Trans. on Electron Devices*, vol. ED-13, No. 1, January 1966, pp. 169–175.

[10] G. I. Haddad, J. R. East and C. Kidner, "Tunnel Transit-Time (TUNNETT) Devices for Terahertz Sources," *Microwave and Optical Technology Letters*, vol. 4, no. 1, January 1991, pp. 23–29.

[11] E. O. Kane, "Zener Tunneling in Semiconductors," *J. Phys. Chem. Solids*, vol. 12, pp. 181-188, 1959.

Table I. Estimated Power Output Including R_s

$f = 100$ GHz

$J_{dc} = 3.1 \times 10^4$ A/cm^2 $V_{dc} = 23.2$ V

Diode Diam. (μm)	Area (cm^{-2})	$R_s(\Omega)$	$-R_d(\Omega)$	$R_L(\Omega)$	V_{RF}(V)	I_{dc}(mA)	P_{dc}(W)	P_{RF} (Gen.) (mW)	P_{RF} (R_L) (mW)	η(%)
20	3.1×10^{-6}	0.63	2.84	2.21	21.6	96	2.23	440	342	15
25	4.9×10^{-6}	0.58	1.82	1.24	21.6	150	3.48	688	468	13
30	7.1×10^{-6}	0.55	1.55	1.0	18.1	216	5.01	830	538	10.7
30	7.1×10^{-6}	1	2	1	14.6	216	5.01	667	333	6.7

Table II. Estimated Power Output Including R_s

$f = 500$ GHz

$J_{dc} = 1.8 \times 10^5$ A/cm^2; $V_{dc} = 6.7$ V

Diode Diam. (μm)	Area (cm^{-2})	$R_s(\Omega)$	$R_L(\Omega)$	$-R_d(\Omega)$	V_{RF}(V)	I_{dc} (mA)	P_{dc} (mW)	P_{RF} (Gen.) (mW)	P_{RF} (R_L) (mW)	η(%)
4	1.26×10^{-7}	2.94	2.9	5.9	3.03	22.7	150	14.6	7.3	4.8
5	1.96×10^{-7}	2.5	2.5	5.0	2.44	35.5	240	18.3	9.2	3.9
7	3.85×10^{-7}	2.0	2.0	4.1	1.71	69.5	470	25.2	12.6	2.7
10	7.85×10^{-7}	1.7	1.7	3.5	1.15	141.9	950	34.6	17.3	1.8

Table III. Estimated Power Output Including R_s
$f = 1000$ GHz
$J_{dc} = 4 \times 10^5$ A/cm^2 $V_{dc} = 4.4$ V

Diode Diam. (μm)	Area (cm^{-2})	$R_s(\Omega)$	$R_L(\Omega)$	$-R_d(\Omega)$	V_{RF}(V)	I_{dc} (mA)	P_{dc} (mW)	P_{RF} (Gen.) (mW)	P_{RF} (R_L) (mW)	η(%)
2	0.31×10^{-7}	7.24	7.24	14.48	0.930	12.47	50	2.5	1.2	2.2
3	0.71×10^{-7}	4.68	4.68	9.36	0.712	28.05	120	4.2	2.1	1.7
4	1.26×10^{-7}	3.7	3.7	7.4	0.556	49.9	220	5.9	2.9	1.3
5	1.96×10^{-7}	3.2	3.2	6.4	0.431	77.9	340	7.1	3.6	1.0

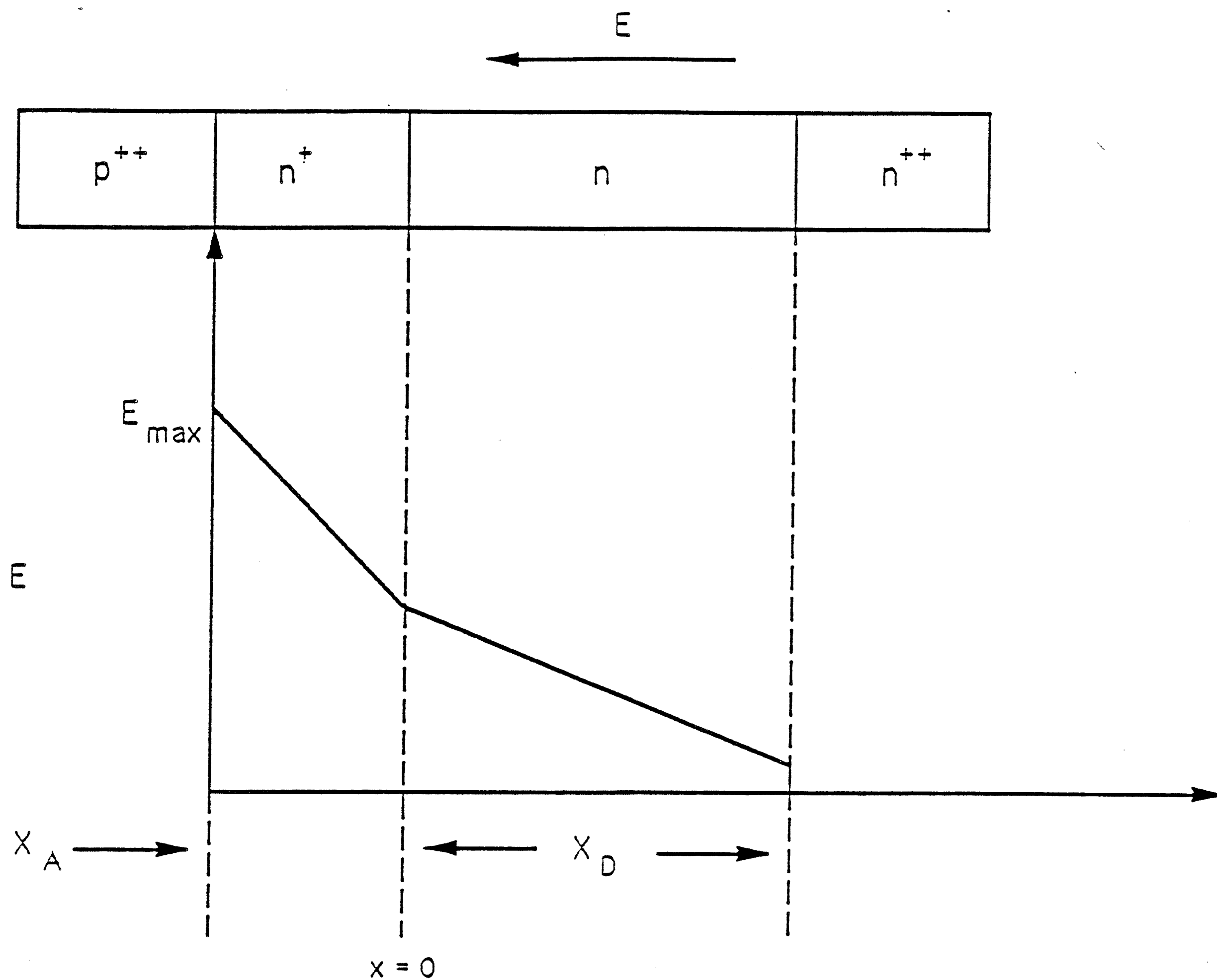

Figure 1. TUNNETT Device Structure and Electric Field Profile.

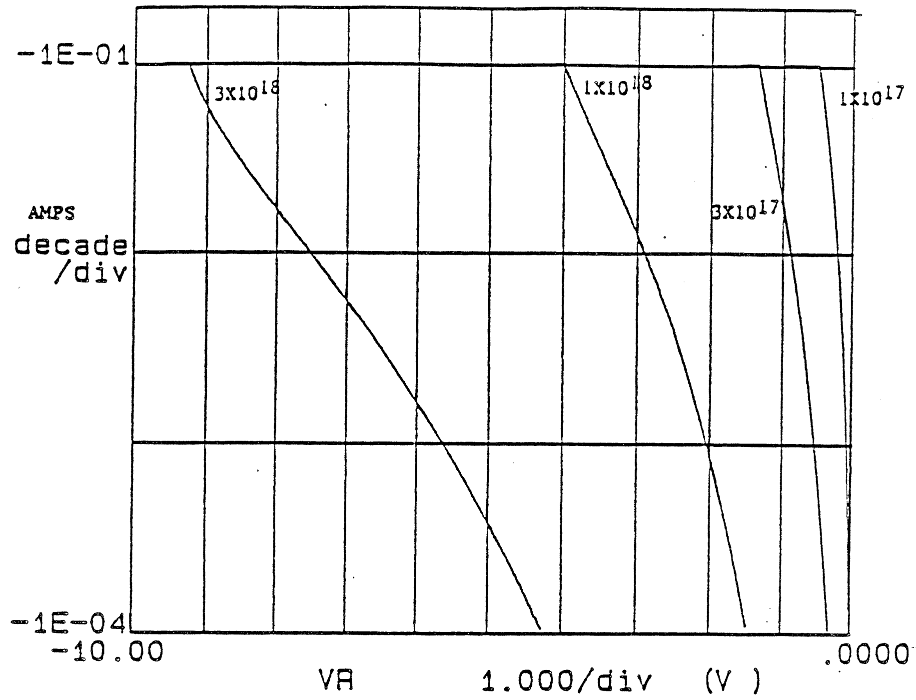

Figure 2. IV Characteristics of MBE Grown p^+n^+ Junctions under Tunnel Breakdown. $p^+ : N_A = 1 \times 10^{19}/cm^3$. From left to right $n^+ : N_D = 3 \times 10^{18}/cm^3$, $1 \times 10^{18}/cm^3$, $3 \times 10^{17}/cm^3$, $1 \times 10^{17}/cm^3$.

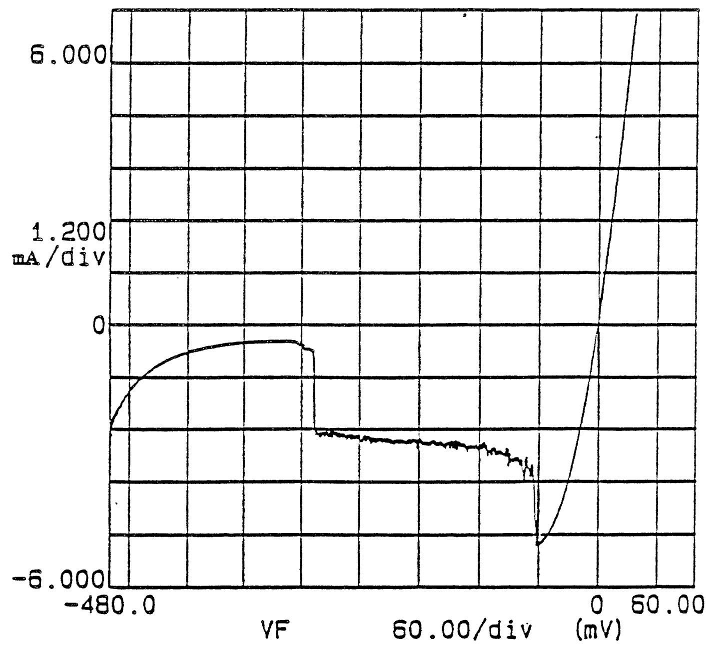

Figure 3. IV Characteristics of Gas Source MBE Grown p^+n^+ Junctions. $p^+ : N_A = 1 \times 10^{19}/cm^3$, $n^+ : N_D = 1 \times 10^{19}/cm^3$.

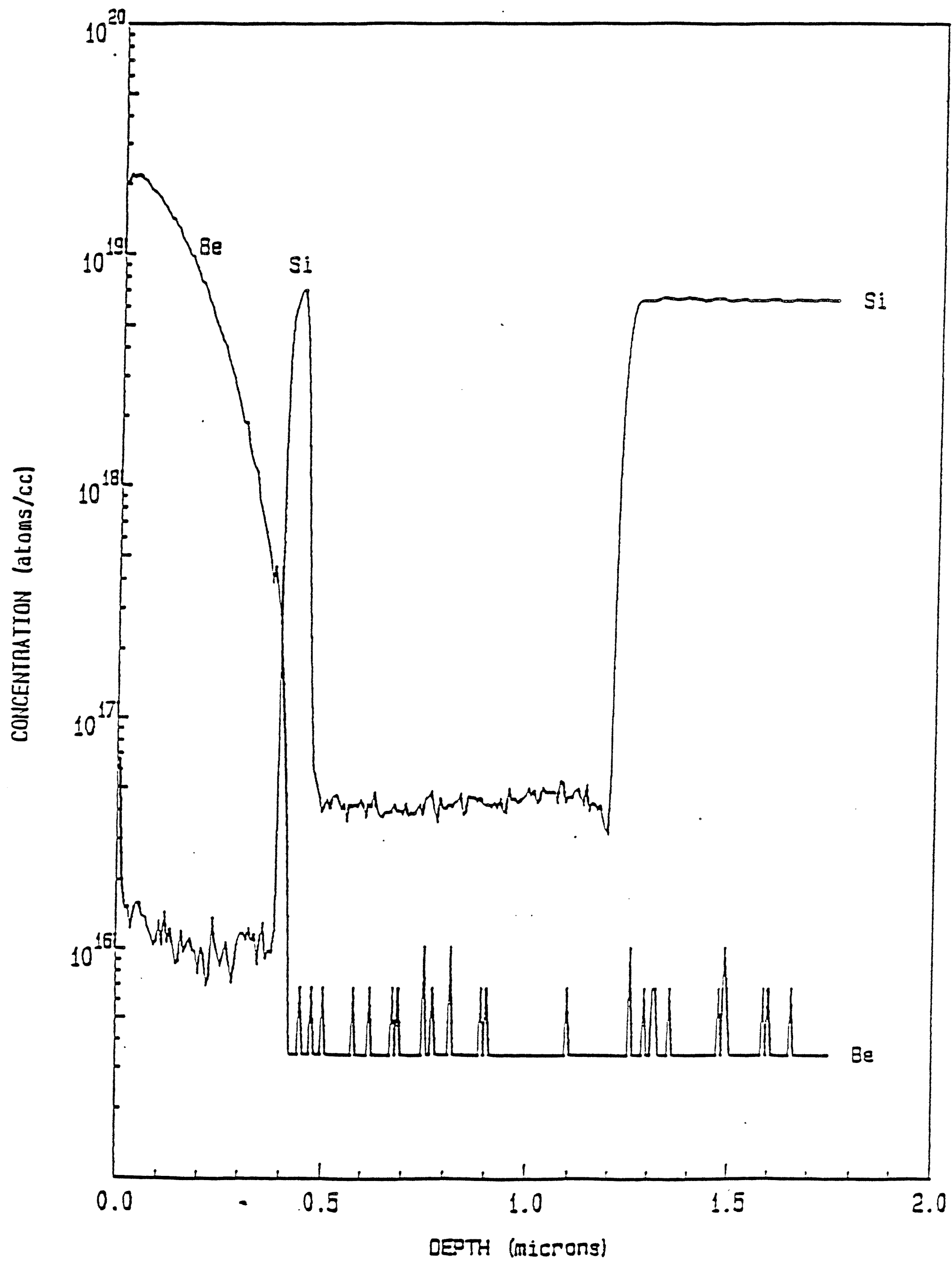

Figure 4. Doping Profile of Nominal TUNNETT Structure Measured using SIMS Analysis (note the excellent Si (n-type) doping profile).

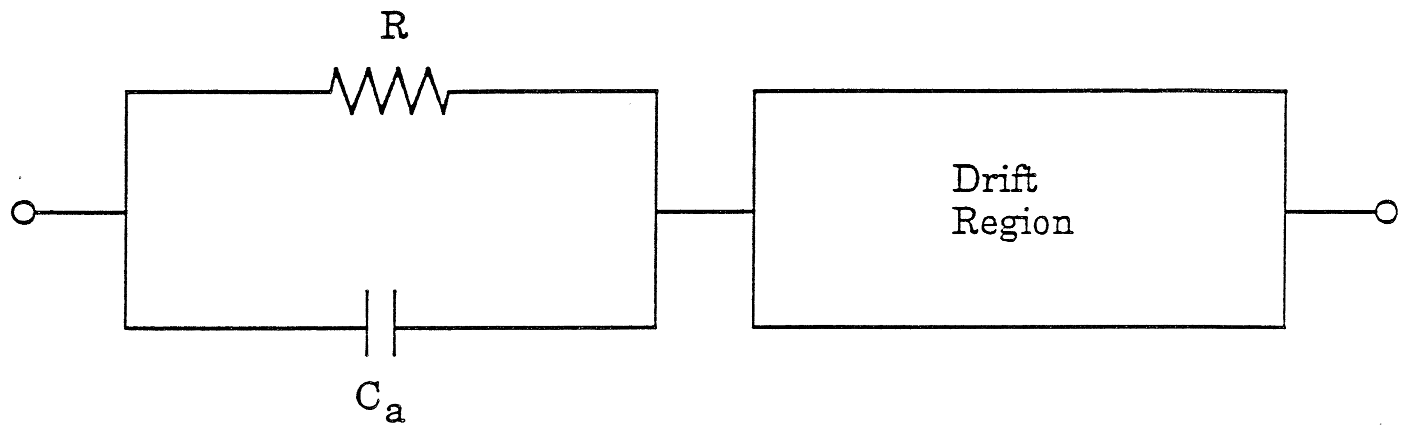

(a)

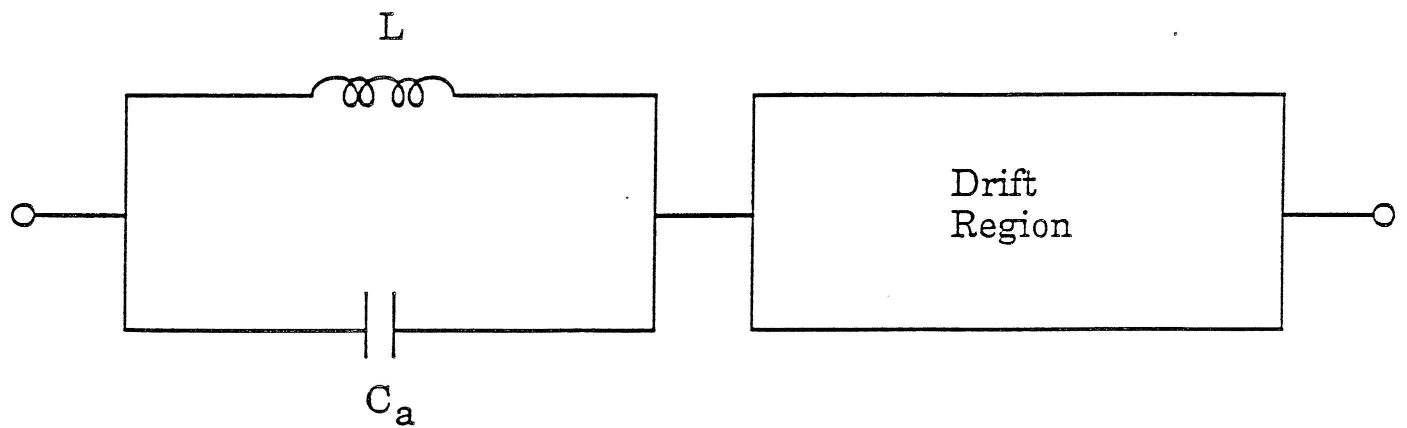

(b)

Figure 5. Small Signal Equivalent Circuit of (a) TUNNETT and (b) IMPATT diodes.

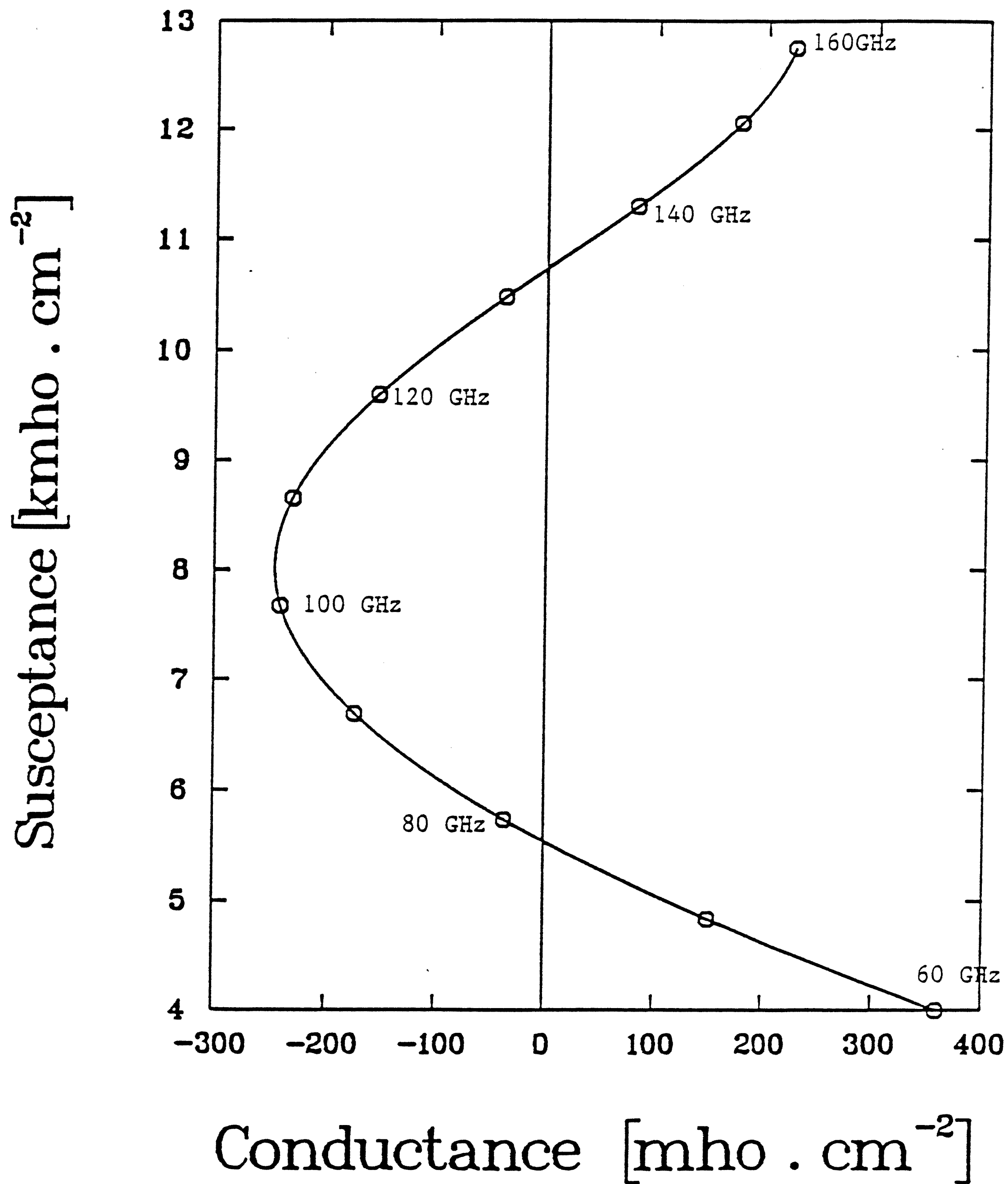

Figure 6. Small Signal Admittance per Square centimeter for a Nominal 100 GHz GaAs TUNNETT Diode using the Injector Described in the Paper (J_{DC}=30kA/cm^2).

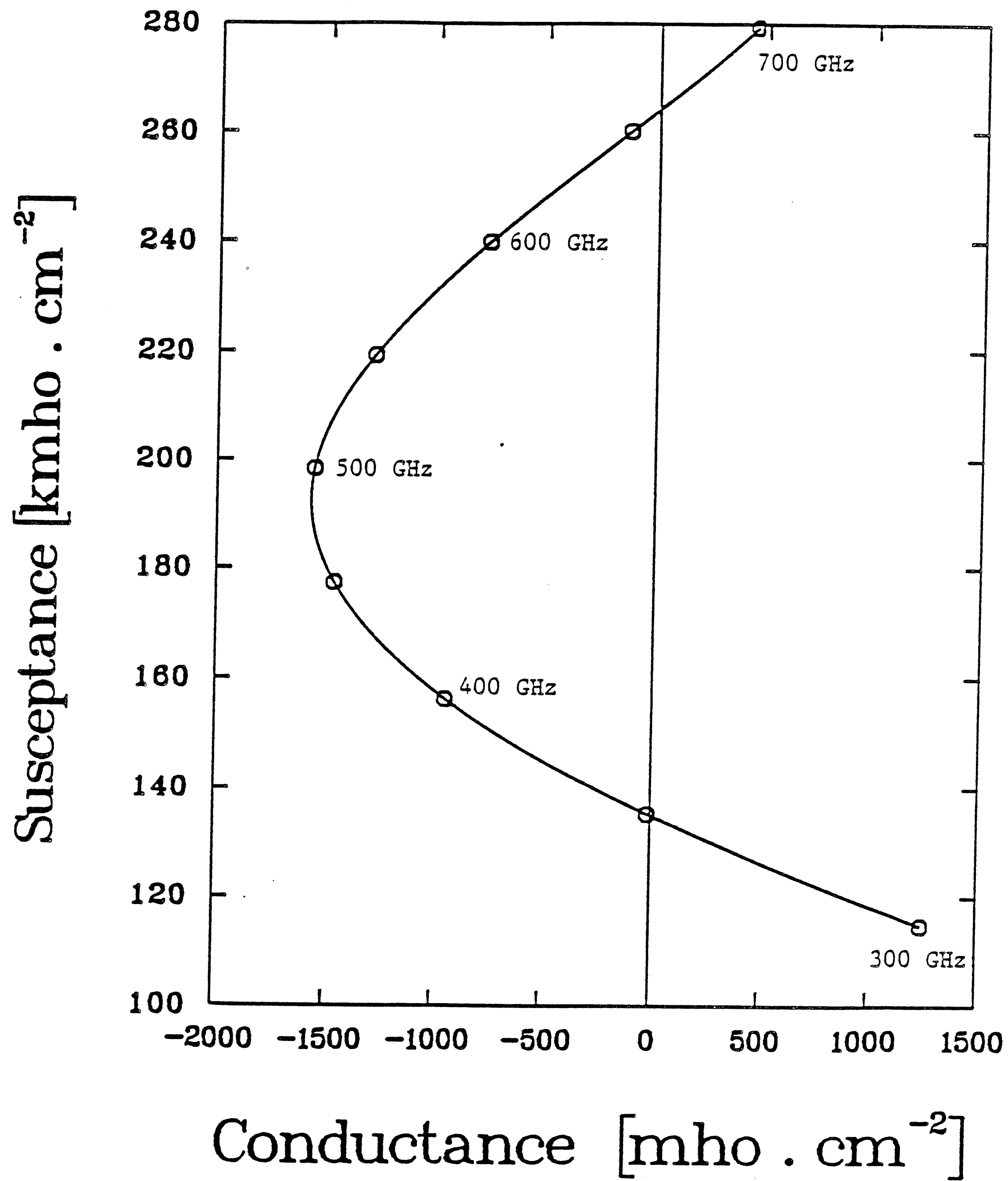

Figure 7. Small Signal Admittance per Square centimeter for a Nominal 500 GHz GaAs TUNNETT Diode using the Injector Described in the Paper (J_{DC}=30kA/cm^2).